E-ISSN: 2583-9667
Indexed Journal
Peer Reviewed Journal
https://multiresearchjournal.theviews.in

Received: 02-06-2023
Accepted: 09-08-2023

INTERNATIONAL JOURNAL OF ADVANCE RESEARCH IN MULTIDISCIPLINARY

Volume 1; Issue 1; 2023; Page No. 522-529

Viscous fluid MHD oscillatory flow through a porous medium in a channel with heat generation and absorption porous medium

[1]Vikash Rai, [2]Dr. Ashfaq Ur Rahman and [3]Dr. Savita Tiwari

[1]Research Scholar, Madhyanchal Professional University, Bhopal, Madhya Pradesh, India
[2, 3]Department of Mathematics, Madhyanchal Professional University, Bhopal, Madhya Pradesh, India

DOI: https://doi.org/10.5281/zenodo.13189203

Corresponding Author: Vikash Rai

Abstract

The main aim of the study is to study the Viscous fluid MHD oscillatory flow through a porous medium in a channel with heat generation and absorption porous medium and examine Thermal radiation and cross-diffusion's impact on heat transfer and hydromagnetic viscous fluid flow adamant parallel plates and learn about the Impact of dual stratification and slip analysis on porous stretched surfaces possible and discuss about the Magnetohydrodynamic copper-water based nanofluid flow between divergent/convergent channel. It is concluded that the fluid movement speeds up as the thermal Grashoff number increases. Increasing the thermal radiation parameter, heat source/sink parameter, and Prandtl number leads to a reduction in the temperature distribution. temperature increases but the concentration profile decreases when the Dufour number and Soret number are improved the Casson parameter, magnetic parameter, and velocity slip parameter reduces fluid velocity at the lower wall, but has the reverse effect near the higher wall.

Keywords: Transportation, channels, thermal conductivity, Casson fluid, velocity

Introduction

A boundary condition must also be put on the field equations to complete the process. The no-slip condition is utilised. As a result of the fact that it is a hypothesis rather than a condition that is derived from a principle of physics, the validity of this hypothesis has been the subject of ongoing discussion in the scientific literature. (2008) According to Wu and Wiwatanapataphee.

Evidences of slip flow of a fluid on a solid surface have been recorded in a variety of different combinations. For instance, conducted research on the flow of polymer solutions in porous media. Their findings demonstrated that the apparent viscosity of the fluids near the wall is lower than that of the fluids in the bulk. As a result, the fluids can demonstrate the phenomenon of apparent slip on the wall. To investigate flow problems involving Newtonian and non-Newtonian fluids with Navier slip boundary condition, a number of different experiments have been carried out.

One definition of the term "nanofluid" describes a liquid suspension that contains particles with a diameter of less than 50 nanometers. The heat transmission capabilities of conventional fluids, such as water, mineral oils, ethylene glycol, motor oil, and so on, are restricted when it comes to applications that include heat transfer. In base fluids, nanofluids are the designed colloidal suspension of nanometer-sized particles of metals and metallic oxides, such as copper, aluminium, iron, gold, and titanium, or their oxides. Nanofluids are distinguished by their nanometer-sized particles. Base fluids may include water, ethylene glycol, oil, bio-liquids, and toluene, among other common examples. The thermal conductivities of base liquids that contain nanoparticles in suspension were found to be much higher than those of base fluids, according to the findings of experimental investigation. Investigation of convective heat transfer in nanofluids has become a topic of contemporary interest since it has applications in a few different fields, such as the operations of power plants, the industrial and transportation industries, the cooling of electronic devices, heat exchangers, and the delivery of nano-drugs. There have only been a few studies to be reported in the literature. Examples of important applications include the production of glass and paper sheets, hot rolling, metallic spiralling, the representation of plastic films, and the extrusion of metals and polymers. The fluid flow that occurs because of a

stretching surface is responsible for these applications. An investigation into the steady boundary layer movement of a nanofluid across a moving semi-infinite plate in a uniform free stream was carried out by Bachok and colleagues using numerical methods. Using heat and mass transfer analysis, a number of researchers have investigated the movement of the boundary layer and the stretching surface of a nanofluid under a variety of different conditions. There are several applications of magnetohydrodynamics in the fields of material processing and engineering. Some examples of these applications are MHD generators, devices used in industry, and nuclear-powered reactors. There is a lot of excitement surrounding the MHD-liquid flow in a spinning tube. Within the confines of an endless rotating porous disc, Hazem investigated the MHD-flow of a viscous, electrically conducting, and incompressible liquid. During the experiment, the liquid was exposed to an external magnetic field that was uniform and perpendicular to the plane of the disc. Following the completion of this work, a few researchers have investigated the effects of MHD on the boundary layer movement and stretching surface of a nanofluid that is subjected to convective heat and mass transfer flow under a variety of conditions.

Literature Review

Abd-Alla, Abdelmooty & Abo-Dahab, Sayed (2023) [2] The peristaltic flow of a Jeffery fluid through a porous media in an asymmetric channel has been investigated in this study. The effects of a magnetic field and heat transfer on the flow of the fluid have been the subject of this investigation. The governing non-linear partial differential equations that characterise the flow model are transformed into linear ones by making use of the necessary non-dimensional parameters. This is done under the premise that the Reynolds number is low and the wavelength is long. There is a presentation of precise answers for the stream function, the pressure gradient, and the temperature. The numerical integration method is utilised in order to compute both the frictional force and the pressure growth. In order to do a parametric analysis, the software MATLAB R2023a is utilised, and the data that is obtained from the study is graphically represented. Every single physical quantity that was taken into consideration was subjected to numerical calculations, which were then graphically portrayed. There is a graphic discussion of the phenomena of trapping. The data that were acquired can be utilised to improve pumping systems in engineering as well as activities related to the gastrointestinal tract. This analysis makes it possible for fluids carried by the body, such as blood and lymph, to circulate freely inside the arteries and veins, which in turn enables oxygen delivery, waste elimination, and other essential components to be carried out.

Majeed, Afraz & Mahmood, Rashid (2023) [3] The purpose of this study is to present the results of an in-depth investigation of the heat and mass transfer characteristics of a Casson fluid flow that passes through a cylinder in a channel that is rippled. As a result of the absence of an analytical solution, the model that is represented by coupled non-linear partial differential equations has been simulated through the utilisation of a higher-order Finite Element Method (FEM). In order to approximate the profiles of velocity, temperature, and concentration, a finite element space that includes the cubic polynomial (P3) is used. On the other hand, the estimation of pressure is carried out by means of a space that contains a quadratic polynomial (P2). A decision of this nature results in a total of ten degrees of freedom for each of the velocity components, temperature, and concentration profile, but only six degrees of freedom are available for the pressure. Linearization of equation systems is accomplished through the application of Newton's technique. A direct solver known as PARDISO is utilised in order to complete the linearized inner system of equations. The results of the computations are presented in the form of velocity, isotherms, and is concentrations, as well as for a number of characteristics of importance, such as the drag and lift coefficients. Over time, it has been shown that the coefficients of drag and lift exhibit a downward tendency when the magnetic parameter M is decreased. Additionally, the drag coefficient has a linear increase trend for all values of Bn. This is due to the fact that fluid forces make up the majority of the drag coefficient at higher values of Bn. In addition, the concentration is highest in the middle of the channel, and it tends to decrease as we get closer to the walls of the channel.

Mohammed, M. (2023) [4] Through the use of the successive linearization technique (SLM), this study explores the flow of micropolar fluid as well as the transmission of heat through a channel that is permeable. A number of characteristics, including coupling, spin-gradient viscosity, and micro-inertia density, are taken into consideration in this work. Through the utilisation of similarity variables, the partial differential equations that are at play are converted into a set of ordinary differential equations. The SLM approach is used to solve the nonlinear equations that are produced as a result, and the correctness and computational efficiency of these equations are validated by comparing them to the results of prior studies. According to the findings of the study, raising the parameters of coupling and spin-gradient viscosity has a beneficial effect on fluid flow, microrotation, heat transfer, and mass transport. This is evidenced by the improved dimensionless profiles. On the other hand, a decrease in these profiles is the result of an increase in the micro-inertia density parameter. This drop can be linked to an increase in the micro-inertia effect of fluid flow and heat transfer, which led to a decrease in convection and a change in the flow pattern in the channel. Consequently, this decline occurred. Furthermore, there is a correlation between increasing Reynolds numbers and decreases in velocity, microrotation, temperature, and concentration dispersion. This indicates that the intensity of the fluid flow will diminish, the heat transfer will be weaker, and the mass transport will be reduced. On the other hand, a larger Peclet number leads to an increase in the temperature and concentration profiles of the fluid, which indicates that thermal convection and mass transport are accelerated significantly. The ramifications of these discoveries are substantial for applications that involve micropolar fluids, such as filtration systems, microchannels, lubrication systems, and blood flow systems.

Tanveer, Anum & Abidin, Zain (2023) [5] Cilia is a mechanism that plays a significant role in the functioning of epithelial cells in the respiratory tract, cerebrospinal flow in the brain, hair bundles in the ear, photoreceptors in the retina, and other structures. In addition, cilia are present in

the fallopian tube of a human being, where they are responsible for transporting sperm, embryos, and ova. As part of this study, we analyse the consequences that are brought about by the combination of magnetic field and mixed convection. Within the scope of this investigation, we provide a description of the flow and heat transfer properties of MHD Carreau fluid in the fallopian tube with metachronal wave of cilia. Under the conditions of creeping phenomena and long wavelength approximation, the mathematical equation depicting the situation is carried out. The NDSolve method of the Mathematica software is utilised in order to acquire the numerical solution for the extra stress tensor, the temperature profile, and the streamline pattern. The final section contains a discussion of the physical and graphical behaviour of various values of the involved parameter. Due to the fact that the diameter of the cilia walls is extremely small, the parametric values are kept at a low level (less than 10).

Boudjemline, Attia & Rehman, Sohail (2023) [9] In high-performance thermal engineering processes, the consideration of heat transfer for non-Newtonian fluid flows between non-parallel wall channels has a significant and long-lasting impact. Over the past few years, this approach has been utilised widely in a wide variety of natural flows and industrial processes. Some examples of these include the flow of blood through human veins, lubrication systems, vehicle radiators, thermal pumps, and water purification processes, among similar applications. Therefore, the purpose of this research is to improve thermal performance by incorporating ultrafine metallic nanoparticles into working fluids. We hope to accomplish this goal. This research effort presents a numerical examination for buoyancy-driven flow of Carreau nanofluids that are confined in a vertical converging enclosure. This inquiry was carried out with the intention of producing this goal. In addition, the examination of heat and mass transfer, together with non-linear thermal radiation and activation energy, is mathematically stated using Buongiorno's model. A new formulation is created for exclusively radial flow within this converging channel, and appropriate non-dimensional variables are utilised for the purpose of simplifying the problem. Following the transformation of these equations, a numerical approach is taken with the use of a flexible numerical method, which is the bvp4c function in MATLAB. The outcomes of the simulation are depicted by virtue of the distributions of nanofluid velocity, temperature, and concentration, with variations in the dimensionless parameters that govern the system. According to the findings, the velocity was dramatically lowered when the activation energy parameter was increased. In addition, the higher values of the Grashof number result in an increase in the intensity of the conduct in velocity distributions.

Abdulridah, Saja & Jasim, Abeer (2023) [7] The Jeffrey Hamel flow problem is investigated in this paper by employing a perturbation iteration technique (PIS) to analyse the flow and heat transfer of a nanofluid through a convergent or divergent channel in a porous media. The channels in question are either convergent or divergent. The nanofluid is constantly moving through the channel as a result of the magnetic field's influence on it. In order to model the motion of various nanofluids, momentum and energy equations are utilised. This allows for the modelling of the motion. There has been discussion over the impact that certain variables, including the opening channel angle, Reynolds number, Darcy number, Hartmann number, Prandtl number, and Eckert number, have on nanofluidic flows that occur through plates that are not parallel to one another. It has been discovered that the viscosity of a fluid improves with an increase in the Reynolds number when the velocity of the fluid increases. The Darcy number causes an increase in flow and an increase in heat transfer, both of which contribute to a decrease in the amount of friction that occurs within the system. In addition, when the results of the other variables were analysed and their impacts on the velocity and temperature profiles were compared with those of comparable research that were published in the literature, a satisfactory level of agreement was discovered. This is evident from the tables and illustrations that are mentioned in this paper, and it also demonstrates that this approach provides us with an excellent study for analysing the Jeffrey Hamel dilemma.

Materials and Methods

Fluid flow between plates is gaining increasing attention due to its wide range of applications in technology and science, including nuclear waste disposal, drying processes, thermonuclear fusion, furnace design, glass production, thermal energy storage, geothermal energy recovery, and flow through filtering devices. Moreover, the study of natural convective flow is highly valued for its industrial, practical, and environmental applications. It is widely used in several fields such as material processing, electronic component cooling, energy system security, thermal regulatory processes, motors, atmospheric fluxes, and air conditioning systems. Studied time-dependent natural convective Couette flow with one stationary plate and another moving in its own plane. examined the impact of mass transfer on free convective flow past an exponentially accelerated vertical plate under constant heat flux. Sreekanth and colleagues (2001) studied time-dependent free convective hydromagnetic flow with dissipation using the finite difference approach. Conducted a quantitative analysis of the mass transfer impact on viscous fluid flow between permeable plates. He analysed the flow while being affected by a transverse magnetic field. discussed 2-D steady laminar flow with permeable slip limits inside a conduit. Studied the magnetohydrodynamic natural flow in a porous media with radiation and cross-diffusion effects. Demonstrated the impacts of magnetic field and mixed convection between stationary parallel vertical plates. Seth and colleagues (2010) studied the time-dependent hydromagnetic movement of a viscous fluid that generates and absorbs heat in a rotating channel, considering non-zero velocity at the boundary.

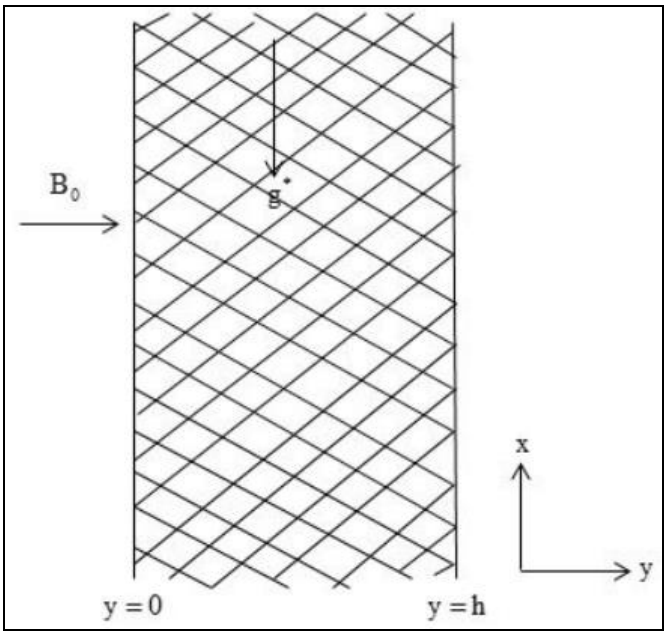

Fig 1: Geometry of the problem

Analysed is a mature dynamic laminar Circular motion of a thick liquid between vertical plates that are parallel. The fluid is electrically conductive, incompressible, and optically thin, with the Cogley approximation used to calculate radiative heat flow. Both packed onto vertical plates with a porous material. They are positioned far away, h as seen in figure 1. The impacts in terms of heat sink/source and magnetic field strength B0 were also examined. Radiative heat transmission occurs between the plates owing to their elevated temperatures.

The equations that control the behaviour of viscous fluids under these circumstances are as follows

$$\frac{\partial u^*}{\partial t^*}=\upsilon\frac{\partial^2 u^*}{\partial y^{*2}}+g^*\beta_T\left(T^*-T_0^*\right)+g^*\beta_C\left(C^*-C_0^*\right)-\frac{\sigma}{\rho}B_0{}^2u^*-\frac{\upsilon}{K_p^*}u^*,$$

$$\rho C_p\frac{\partial T^*}{\partial t^*}=\kappa\frac{\partial^2 T^*}{\partial y^{*2}}-\frac{\partial q_r}{\partial y^*}-Q_0\left(T^*-T_0^*\right),$$

$$\frac{\partial C^*}{\partial t^*}=D\frac{\partial^2 C^*}{\partial y^{*2}},$$

as a result of which limits -

$$u^*\left(y^*,t^*\right)=U_0\left(1+\varepsilon e^{i\omega^* t^*}\right),T^*\left(y^*,t^*\right)=T_1^*+\varepsilon\left(T_1^*-T_0^*\right)e^{i\omega^* t^*},C^*\left(y^*,t^*\right)=C_1^*\text{ at }y^*=0,$$

$$u^*\left(y^*,t^*\right)=0,T^*\left(y^*,t^*\right)=T_1^*,C^*\left(y^*,t^*\right)=C_0^*\text{ at }y^*=h.$$

Here are the definitions of the variables: u∗ (axial velocity), t∗ (time), υ (kinematic viscosity), g* (acceleration due to gravity), βT (coefficient of thermal expansion), βC (coefficient of solutal expansion), T∗ (fluid temperature), T0* (free stream's reference temperature), C∗ (fluid's concentration), C0* (concentration of the species at wall), Kp* (porous medium's permeability), σ (electrical conductivity), ρ (density of the fluid), Cp (specific heat at constant pressure), κ (thermal conductivity), rq (radiative heat flux), Q0 (heat generation/absorption constant), D (mass diffusing coefficient), U0 (mean velocity), ω* (frequency of the oscillation), ε (constant), C1* (concentration), and T_1* (temperature).
Applying the Cogley *et al*. (1968) [13] approach in a low-density thin fluid.

$$\frac{\partial q_r}{\partial y^*}=4\left(\alpha^*\right)^2\left(T^*-T_0^*\right),$$

here "α* is Cogley mean absorption coefficient".
So decreases in the energy equation as:

$$\rho C_p\frac{\partial T^*}{\partial t^*}=\kappa\frac{\partial^2 T^*}{\partial y^{*2}}-4\left(\alpha^*\right)^2\left(T^*-T_0^*\right)-Q_0\left(T^*-T_0^*\right),$$

Here we are presenting some dimensionless quantities as:

$$y=\frac{y^*}{h},t=\frac{t^*\upsilon}{h^2},\omega=\frac{\omega^* h^2}{\upsilon},u=\frac{u^*}{U_0},\theta=\frac{T^*-T_0^*}{T_1^*-T_0^*},\phi=\frac{C^*-C_0^*}{C_1^*-C_0^*}.$$

The use of boundary conditions and equations into governing equations allows us to get –

$$\frac{\partial u}{\partial t}=\frac{\partial^2 u}{\partial y^2}+Gr_T\theta+Gr_C\phi-\left(M^2+K_p\right)u,$$

$$Pr\frac{\partial\theta}{\partial t}=\frac{\partial^2\theta}{\partial y^2}-\left(Rd+Hs\right)\theta,$$

$$Sc\frac{\partial\phi}{\partial t}=\frac{\partial^2\phi}{\partial y^2},$$

With

$$y=0:u\left(y,t\right)=1+\varepsilon e^{i\omega t},\theta\left(y,t\right)=1+\varepsilon e^{i\omega t},\phi\left(y,t\right)=1,$$

$$y=1:u\left(y,t\right)=0,\theta\left(y,t\right)=1,\phi\left(y,t\right)=0.$$

The variables referred to are: thermal Grashoff number (GrT), solutal Grashoff number (GrC), porosity parameter (Kp), magnetic parameter (M), radiation parameter (Rd), heat source/sink parameter (Hs), Prandtl number (Pr), and Schmidt number (Sc). The following are defined as:

$$Gr_T=\frac{g^*\beta_T h^2\left(T_1^*-T_0^*\right)}{\upsilon U_0},\quad Gr_C=\frac{g^*\beta_C h^2\left(C_1^*-C_0^*\right)}{\upsilon U_0},\quad K_p=\frac{h^2}{K_p^*},\quad M^2=\frac{\sigma B_0{}^2 h^2}{\rho\upsilon},$$

$$Rd=\frac{4\left(\alpha^*\right)^2 h^2}{\kappa},\ Hs=\frac{Q_0 h^2}{\kappa},\ Pr=\frac{\rho\upsilon C_p}{\kappa},\ Sc=\frac{\upsilon}{D}.$$

Results and Discussion

Figure 2 illustrates how the flow profile is affected by the thermal Grashoff number. An increase in the thermal Grashoff number leads to an augmentation in the velocity

profile. Fluid velocity briefly increases in the boundary layer area. The boundary forces accelerate the fluid by acting as a favourable pressure gradient inside the boundary layer. Therefore, the thickness of the boundary layer increases. Figure 3 demonstrates the impact of the porosity parameter on the velocity profile, indicating that an increase in the porosity parameter results in a reduction in the fluid flow profile. Higher values of the porosity parameter lead to increased flow restriction in the direction of flow, resulting in a reduction in velocity.

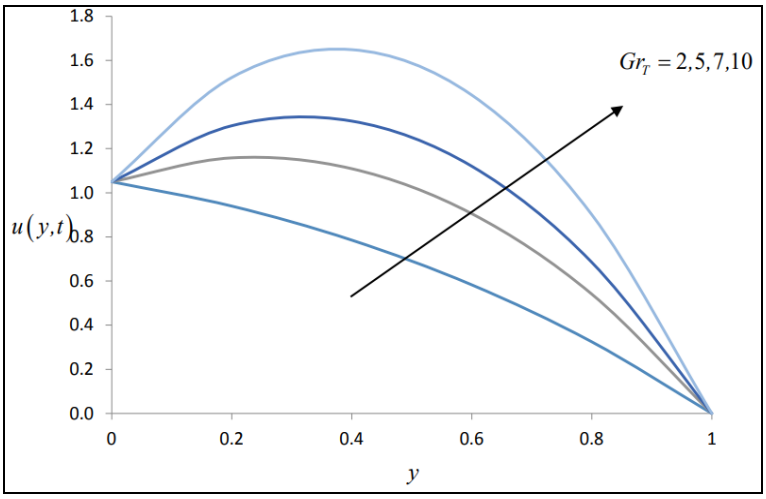

Fig 2: Effect of thermal Grashoff number GrT on velocity profile u yt (,) when Kp = 0.09, M =1, GrC = 0.1, Rd = 0.25, Hs = 0, Pr = 0.7, ω = 0.5, ε = 0.1"

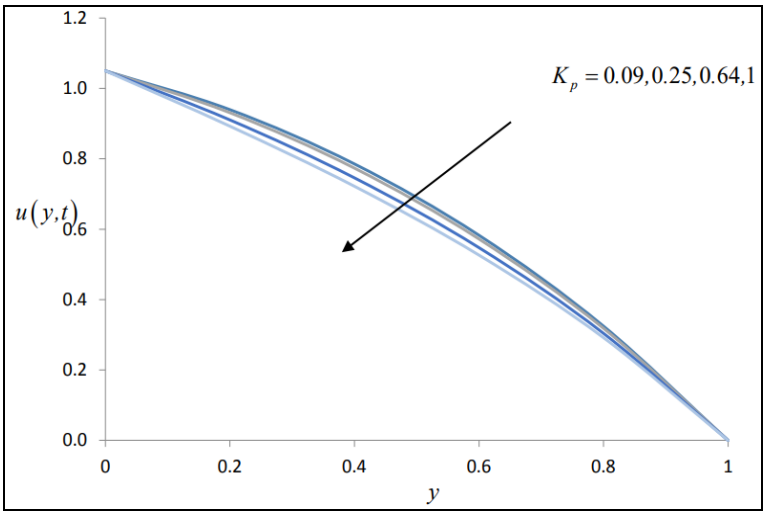

Fig 3: Effect of porosity parameter Kp on velocity profile u yt (,) when M =1, GrT = 2, GrC = 0.1, Rd = 0.25, Hs = 0, Pr = 0.7, ω = 0.5, ε = 0.1.

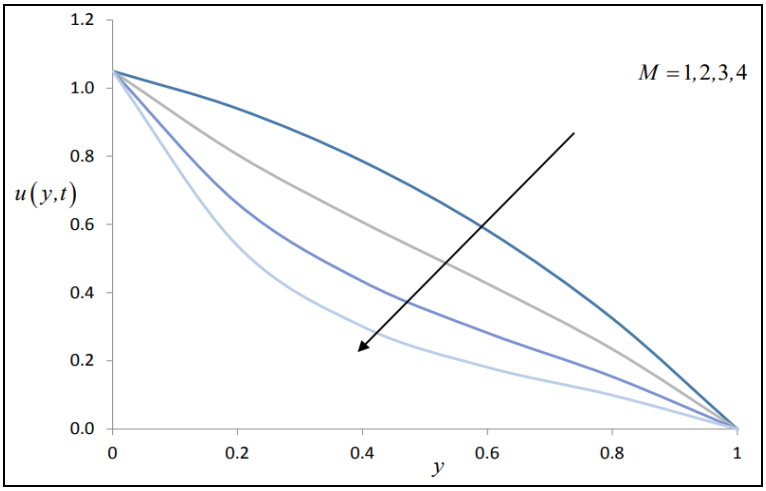

Fig 4: Effect of magnetic parameter M on velocity profile u yt (,) when Kp = 0.09, GrT = 2, GrC = 0.1, Rd = 0.25, Hs = 0, Pr = 0.7, ω = 0.5, ε = 0.1.

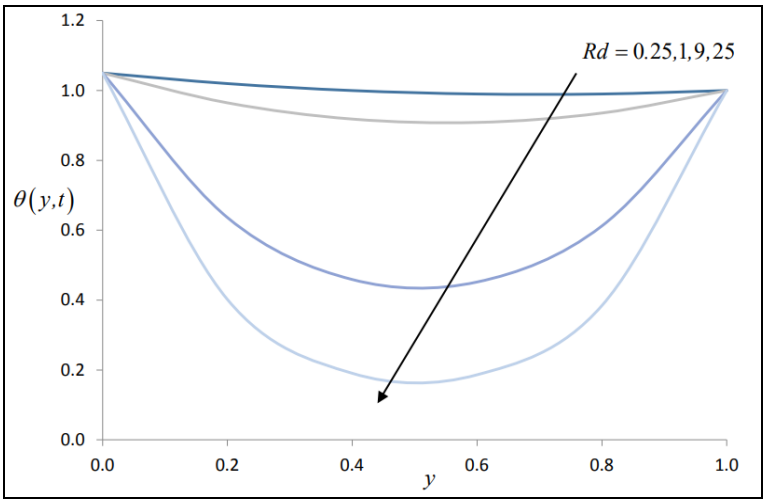

Fig 5: Effect of radiation parameter Rd on temperature profile θ (yt,) when Kp = 0.09, M =1, GrT = 2, GrC = 0.1, Hs = 0, Pr = 0.7, ω = 0.5, ε = 0.1.

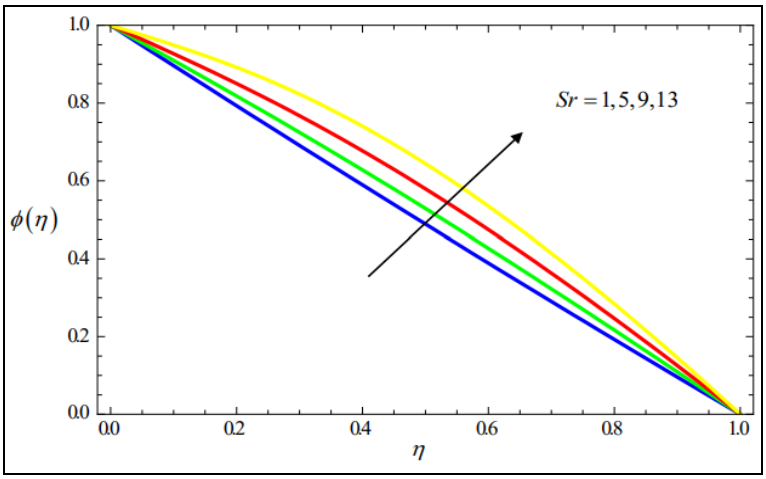

Fig 6: Effect of Sorbet number Sr on concentration profile φ (η) when Re = 5, M =1, Rd = 2, Pr = 2, Df = 0.5, Sc = 0.1, K = 0.5, β s = 0.3, R = 0.3.

Table 1: Average residual errors at 20th order of approximations when Re = 5, M =1, Rd = 0.5, Pr =1, Df = 0.5, Sc = 0.1, K = 0.5, Sr = 0.5, β s = 0.3, R = 0.3".

m (order of estimations)	*Ef, m*	*Eg, m*	*Eθ, m*	*Eϕ, m*
4	2.19607×10^{-5}	1.03836×10^{-6}	4.55299×10^{-7}	1.27078×10^{-8}
8	3.00678×10^{-12}	1.23058×10^{-12}	6.80472×10^{-14}	1.71917×10^{-15}
12	4.84855×10^{-18}	1.82215×10^{-18}	2.82916×10^{-20}	1.85228×10^{-21}
16	5.33996×10^{-24}	3.41073×10^{-24}	2.91909×10^{-26}	1.64732×10^{-27}
20	1.79547×10^{-25}	5.82138×10^{-27}	3.92317×10^{-27}	4.67134×10^{-29}

Table 2: The convergence control parameters $\hbar_f$, $\hbar_g$, $\hbar_\theta$, and $\hbar_\phi$ at 8th order of approximations for velocity, temperature, and concentration profiles when Re = 5, M =1, Rd = 0.5, Pr = 0.1, Df = 0.2, Sc = 0.1, K = 0.5, Sr = 0.2, β s = 0.3, R = 0.3".

Order of estimations	$\hbar_f$	$\hbar_g$	$\hbar_\theta$	$\hbar_\phi$	$(E_m)Total$
2	-0.900742	-0.904863	-0.554332	-0.934472	8.25003×10^{-2}
4	-0.886684	-0.940772	-0.617104	-1.033150	2.29982×10^{-5}
6	-0.884652	-0.903183	-0.617277	-1.034750	7.78014×10^{-9}
8	-0.879274	-0.849587	-0.683871	-0.845214	2.53317×10^{-12}

Table 3: Convergence of HAM solutions when Re = 5, M =1, Rd = 0.5, Pr =1, Df = 0.5, Sc = 0.1, K = 0.5, Sr = 0.5, β s = 0.3, R = 0.3".

Order of estimations	$-f''(0)$	$-g''(0)$	$-\theta'(0)$	$-\phi'(0)$
5	3.7354622652	0.3277613141	1.3182542526	1.0536286341
10	3.7354762061	0.3277627151	1.3182545820	1.0536253551
15	3.7354762045	0.3277627145	1.3182545828	1.0536253551
20	3.7354762045	0.3277627145	1.3182545828	1.0536253551
30	3.7354762045	0.3277627145	1.3182545828	1.0536253551
40	3.7354762045	0.3277627145	1.3182545828	1.0536253551
50	3.7354762045	0.3277627145	1.3182545828	1.0536253551
60	3.7354762045	0.3277627145	1.3182545828	1.0536253551

Table 4: Comparison of the values of – f'' (0) and −g'' (0) at different orders when Re = 5, Rd = 0.5, Pr =1, Sc = 0.1, β s = 0.5, R = 0.5, M = 0, Df = 0, K = 0, Sr = 0".

Order of approximations	Present results		"Hayat *et al*. (2014) [12]"	
	$-f''(0)$	$-g''(0)$	$-f''(0)$	$-g''(0)$
5	2.9904573244	0.5037507210	2.987025	0.503715
10	2.9905251277	0.5037629045	2.990508	0.503763
15	2.9905251497	0.5037629113	2.990524	0.503762
20	2.9905251497	0.5037629113	2.990525	0.503762
25	2.9905251497	0.5037629113	2.990525	0.503762

Figures 3 and 4. show that increasing the magnetic parameter leads to a decrease in the velocities ' f and ' g of the fluid in the lower part of the channel due to the resistive force known as Lorenz force generated by the magnetic field, which hinders the fluid movement. However, the velocities f and g exhibit contrasting behaviour in the top and lower regions owing to continuous fluid input at the upper wall causing cross-flow and resulting in increased velocity. Figure 3. illustrates the increase in temperature as the radiation parameter increases. A greater radiation parameter results in more heat transfer to the fluid, leading to an enhanced temperature profile. Figure 3. shows that when the Prandtl number increases, the fluid temperature decreases. An increase in Prandtl number results in decreased heat diffusivity and increased momentum diffusivity. This fluctuation in thermal diffusivity and momentum diffusivity suggests a decrease in the thickness of the thermal boundary layer and the temperature of the fluid. An increase in the Dufour number improves the temperature profile and decreases the concentration distribution, as seen in figures 4. The Dufour number quantifies the impact of heat flow resulting from a concentration gradient. An increase in the Dufour number results in heat generation in the fluid, leading to an increase in temperature. Figure 4. shows that when the Schmidt number increases, the concentration field drops due to the reduction in mass diffusivity, leading to a decrease in the thickness of the concentration boundary layer. An increase in the chemical reaction parameter results in a decrease in the concentration profile seen in figure 4. Figures 5 and 6 depict the temperature and concentration profiles as they vary with various Soret number values. Figure 5 illustrates that the temperature lowers with an increase in the Soret number due to the Soret number reducing the thickness of the thermal boundary layer. An increase in the Soret number leads to a higher concentration profile due to the Soret number's ability to enhance concentration flux, as shown in figure 6. Table 1. displays the average residual errors at the 20th order of approximations for each differential equation. The table shows that the residual errors decrease consistently as the order of approximation increases. Table 2. displays the numerical values of convergence control parameters. Table 3 displays the convergence of the HAM method up to the 60th order of approximations. We validated the results of our research by comparing them with the findings presented in the literature by Hayat *et al*. (2014) [12]. They are in a remarkable agreement and shown in table 4.

Conclusion

- Temperature profile decreases with radiation parameter and increases with Prandtl number and Eckert number.
- An increase in temperature and a reduction in concentration are noticed due to an increase in thermophoresis and Brownian motion parameters.
- The temperature increases but the concentration profile decreases when the Dufour number and Soret number are improved.
- The Schmidt number and chemical reaction parameter decrease the concentration profile.
- Increasing the Casson parameter, magnetic parameter, and velocity slip parameter reduces fluid velocity at the lower wall, but has the reverse effect near the higher wall.
- Increasing the squeezing parameter leads to a higher velocity but decreases the heat and mass transfer rate.
- The Darcy number increases fluid velocity at the lower wall and decreases it at the top wall.
- The temperature of the fluid rises as the radiation parameter, Eckert number, and Dufour number increase.
- Temperature falls under the influence of Casson parameter, thermal slip parameter, Prandtl number, thermal stratification parameter, and Soret number.
- The concentration profile increases with the Soret number and decreases with the chemical reaction parameter, solutal stratification parameter, Dufour number, solutal slip parameter, and Schmidt number.
- Higher micropolar parameter and Darcy number values lower fluid velocity F (η) at the bottom wall and raise it at the top wall.

References

1. Maciejewska B, Hozejowska S, Grabowski M, Poniewski M. Numerical analysis of the boiling heat transfer coefficient in the flow in mini-channels. Acta Mechanica et Automatica. 2023;17:595-604. Available from: https://doi.org/10.2478/ama-2023-0069
2. Abd-Alla A, Abo-Dahab S, Salah D, Bayones F, Abdelhafez M. Magneto-hydrodynamic peristaltic flow of a Jeffery fluid in the presence of heat transfer through a porous medium in an asymmetric channel. Scientific Reports. 2023;13(1):21088. Available from: https://doi.org/10.1038/s41598-023-48137-x
3. Majeed A, Mahmood R, Shahzad H, Pasha A, Raizah Z, Hosham H, *et al*. Heat and mass transfer characteristics in MHD Casson fluid flow over a cylinder in a wavy channel: higher-order FEM computations. Case Studies in Thermal Engineering. 2023;42:102730. Available from: https://doi.org/10.1016/j.csite.2023.102730
4. Mohammed M. Micropolar flow and heat transfer within a permeable channel using the successive linearization method. Open Physics. 2023;21. Available from: https://doi.org/10.1515/phys-2023-0177
5. Tanveer A, Abidin ZU, Duraihem FZ, Saleem S. Flow and heat transfer characteristics in fallopian tube with metachronal wave of cilia. Journal of Mechanics. 2023;39:385-394. Available from: https://doi.org/10.1093/jom/ufad027
6. Boudjemline A, Rehman S, Ali H, ben Khedher N. Analysis of flow and heat transport between converging channels. The European Physical Journal Special Topics. 2023:6:1-7. Available from: https://doi.org/10.1140/epjs/s11734-023-00806-8
7. Abdulridah S, Jasim A. New analytical study of heat transfer analysis of Jeffery–Hamel nanofluid flow problem with porous medium. Journal of Advanced Research in Fluid Mechanics and Thermal Sciences. 2023;103:105-32. Available from: https://doi.org/10.37934/arfmts.103.1.105132
8. Yadav PK, Yadav N. A study on the flow of couple stress fluid in a porous curved channel. Computers & Mathematics with Applications. 2023;152:1-15. Available from: https://doi.org/10.1016/j.camwa.2023.10.004
9. Rehman KU, Shatanawi W, Çolak AB. Artificial neural networking magnification for heat transfer coefficient in convective non-Newtonian fluid with thermal radiations and heat generation effects. Mathematics. 2023;11(2):342.
10. Bilal S, Shah IA, Ghachem K, Aydi A, Kolsi L. Heat transfer enhancement of MHD natural convection in a star-shaped enclosure, using heated baffle and MWCNT–water nanofluid. Mathematics. 2023;11(8):1849.
11. Noranuar WN, Mohamad AQ, Shafie S, Jiann LY. Heat and mass transfer on Magnetohydrodynamics Casson carbon nanotubes nanofluid flow in an asymmetrical channel via porous medium. Symmetry. 2023;15(4):946.
12. Imran M, Hayat S, Mailk MY. On topological indices of certain interconnection networks. Applied Mathematics and Computation. 2014;244:936-951.
13. Cogley DR, Butler JN. The activity of lithium in lithium amalgams. The Journal of Physical Chemistry. 1968;72(3):1017-1020.